Deciphering Flood Event Information from Tree-Ring Data in the Tatra Mountains: Implications for Hazard Assessment

Juan Ballesteros-Cánovas, Barbara Spyt, Karolina Janecka, Ryszard J. Kaczka and Markus Stoffel

Abstract Mountains and their foothills are areas where intense floods are characterized by high discharge and where they occur more often than in lowlands. Furthermore, due to the fact that they are mainly caused by short-lasting heavy rainfall events, they are difficult to predict. The dense network of meteorological stations and river gauges is crucial to understand hydrological processes and to forecast floods. Most mountain regions suffer from a scarcity of instrumental data that are long enough for scientific purposes. In such cases where historical data or instrumental records are lacking, floods in forested catchments can be analysed by using growth series from trees growing along stream channels. In the streams draining the northern slopes of the Tatra Mountains, it was possible to reconstruct the occurrence and magnitude of paleofloods using tree-ring data. More than 1100 increment cores were sampled from 218 *Picea abies* and *Abies alba* trees growing at 6 stream sectors and allowed determination of 480 growth disturbances and a definition of the magnitude of 47 flood events between A.D. 1866 and 2012. In this region, floods are triggered by intense and prolonged rainfall events in spring and

J. Ballesteros-Cánovas (✉) · M. Stoffel
Climatic Change and Climate Impacts, Institute for Environmental Sciences, University of Geneva, 1227 Carouge, Switzerland
e-mail: juan.ballesteros@dendrolab.ch

M. Stoffel
e-mail: markus.stoffel@dendrolab.ch

J. Ballesteros-Cánovas · M. Stoffel
Dendrolab.ch, Institute of Geological Sciences, University of Bern, 3012 Bern, Switzerland

B. Spyt · K. Janecka · R.J. Kaczka
Faculty of Earth Sciences, University of Silesia, 40007 Katowice, Poland
e-mail: barbaraspyt@wp.pl

R.J. Kaczka
e-mail: kaczka@wnoz.us.edu.pl; ryszard.kaczka@us.edu.pl

M. Stoffel
Department of Earth and Environmental Sciences, University of Geneva, 1205 Geneva, Switzerland

Z.W. Kundzewicz et al. (eds.), *Flood Risk in the Upper Vistula Basin*, GeoPlanet: Earth and Planetary Sciences, DOI 10.1007/978-3-319-41923-7_12

summer. These paleoflood records also allowed construction of a regional flood analysis and to reduce the uncertainties in the flood frequency assessment.

Keywords Dendrochronology · Proxy data · Flood information · Hazard assessment

1 Introduction

Floods are one of the most common natural processes worldwide. In mountain streams, the catchment predisposition and steep channel characteristics contribute to a quick hydrological response of catchment and very powerful channel responses. Floods in mountain streams, therefore, are characterized by recurrent, highly-turbulent and sediment-laden flows (Wohl 2000, 2006). These characteristics make mountain streams highly hazardous and flood events therein difficult to forecast (Borga et al. 2011, 2014). Floods in mountain environments have caused large amounts of losses and fatalities in the past, with dramatic and recurrent episodes in all mountain ranges worldwide (Weingartner et al. 2003; Kundzewicz et al. 2014a).

The scientific-technical analyses of floods in mountains require long-term records on both occurrence and flow magnitude (Brázdil et al. 2006). However, the widespread and characteristic scarcity of instrumental data and basic hydrological information in mountain terrains clearly hampers these analyses. Augmenting information about past flood events by using historical archives and indirect evidence in the paleorecord is therefore critical to assess flood hazard, evaluate discharge trends or decipher a link to climate change. Paleoflood records based on tree-ring analyses are, therefore, highly convenient in forested mountain terrains (Ballesteros-Cánovas et al. 2015a, b). The interaction between floods and vegetation growing along a mountain stream can leave datable evidence of past floods in tree rings, which allows tracking of past process activity with high spatial and temporal accuracy. Before the formal definition of paleohydrology (Baker 2008), Sigafoos (1964) already stated that the information contained in tree-ring records of riverine trees is unique and constitutes a valuable source of data for hydrological analysis (Ballesteros-Cánovas et al. 2014). Since then, several efforts have been done to improve the tree-ring analyses to determine past flood records (Ballesteros-Cánovas et al. 2015b for a recent review). All these experiences support the initial hypothesis launched by Sigafoos (1964) about the economic value of tree-rings records for paleoflood analyses, specifically in ungauged or poorly gauged sites. However, a pedagogic explanation about the utility of this kind of information is still needed within the hydrological community (Baker 2008).

Particularly in the Tatra Mountains, flood risk is an important issue and has been a known problem for long time. However, despite the fact that first gauging stations were installed in several streams and rivers in the Tatra Mountains foreland in the late 19th century, a lack of flood processes interpretation is still recognized because of the highly fragmented and incomplete gauging network in the region (Fig. 1).

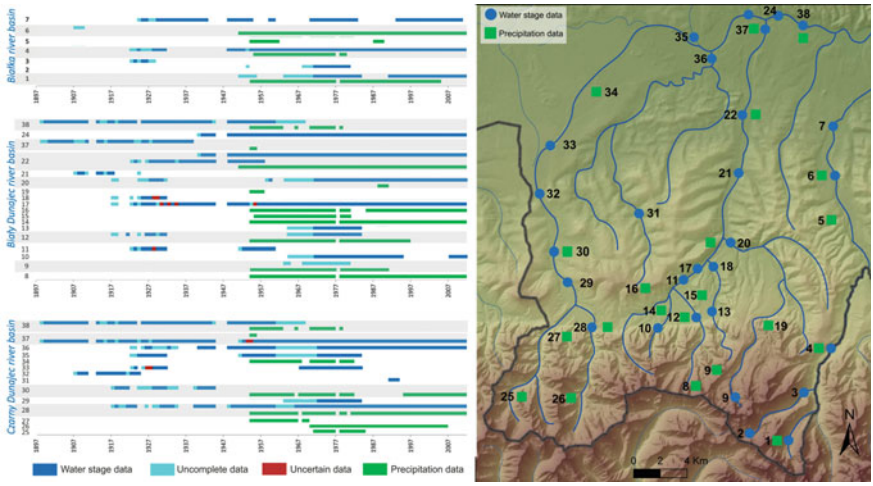

Fig. 1 Spatial and temporal distribution of meteorological and flow gauge dataset on the northern slope and foothills of the Polish Tatra Mountains. After Ballesteros-Cánovas et al. (2015a), published by permission of Elsevier

This problem is even larger as some crucial gauging stations have been relocated after the occurrence of intense flood events (e.g., in 1934), which destroyed several stations and prevented direct data comparison. Moreover, the political and administrative instability of the region—related to both World Wars—also resulted in several gauging network changes and significant losses of records (Szczepański et al. 1996).

Here we synthesize the major research outcomes obtained during the Florist project and report on the use of tree-ring series to decipher the flood history of the Tatra Mountains. We first present the foundation of paleoflood research based on tree rings, provide some fundamental bibliography and then summarize some of the key findings of Ballesteros-Cánovas et al. (2015a, 2016) dealing with the flood dating and peak discharge reconstruction in the region.

2 Fundamentals of Tree-Ring-Based Paleoflood Reconstructions

The methodological basis of paleoflood reconstructions based on tree rings is based on the "process–event–response" concept defined by Shroder (1978). This concept defines the *process* as any geomorphic agent, in this specific case floods, the *event* as a specific impact which the process can induce to a tree; and the *response* the tree's reaction to this specific disturbance. The main disturbances caused by floods include impact scars, tilted stems and abnormal stem morphologies, eroded roots,

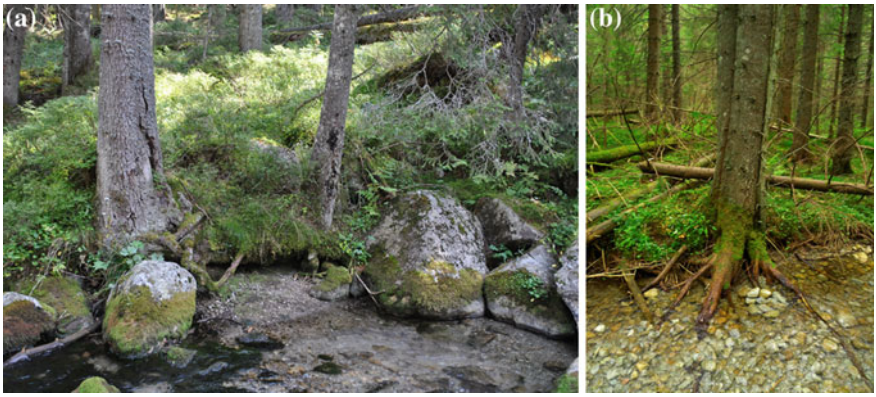

Fig. 2 Examples of main dendrogeomorphic evidence related with floods in the Tatra Mountains: **a** scar on trees and **b** exposed roots

re-sprouting and anatomical abnormalities caused by prolonged inundation without needed to invoke mechanical damages (Stoffel and Bollschweiler 2009; Stoffel et al. 2010; Stoffel and Corona 2014). Hydrological processes also control riparian vegetation pattern; these have been used to understand the frequency and duration of flooding events (Kozlowski 2002; Kames et al. 2016).

At the level of forest stands, flood activity modulates the riparian forest. Extreme flood events may eliminate trees along the channel and flood plain. Survivor trees may benefit from less competition, more light, nutrients and water availability (Osterkamp et al. 2012; Stoffel and Wilford 2012). At the same time, new plants may germinate on bare surfaces. These vegetation changes condition the growth rate and the age structure of the forest, which has been used to date the minimum age of new landforms and its linkage with fluvial dynamic (Sigafoos 1964).

At the scale of individual trees, and in the case of Tatra Mountain streams, we most commonly observe mechanical damage in the form of stem wounds (Fig. 2a). Previous studies have reported that in this region, the transport of boulders and woody debris during intense flood events can impact trees, removing the bark and destroying the meristematic cambium tissue (Zielonka et al. 2008). Scars on trees can, however, also be generated by falling trees or impacts during logging, which is quite widespread in the region. After wounding, trees react upon this disturbance by compartmentalizing the wounded surface (Stoffel and Klinkmüller 2013; Ballesteros et al. 2014) so as to minimize rot and decay. Therefore, the partial removal of bark and cambium tissues during mechanical wounding will favor the formation of callus pads at the edge of open wounds and dissimilar growth disturbances according to tree species.

Conifers growing in the Tatras Mountains respond to wounding in a way which allows them to minimize the risk of cell embolism and cavitation and by forming smaller cells. In addition, *Abies*, *Larix* and *Picea* have been reported to form tangential rows of traumatic resin ducts (TRD) after mechanical disturbance (Stoffel

2008; Schneuwly et al. 2009a, b; Ballesteros et al. 2010a), as well as a significant reduction of both ring width and the size of the lumen of earlywood tracheid (Arbellay et al. 2012a, b; Ballesteros-Cánovas et al. 2010a). Specifically, TRDs normally form tangentially within the current growth ring and close to the wound, but can also be observed in subsequent rings (Bollschweiler et al. 2008; Stoffel and Hitz 2008). This anatomical feature represents a nonspecific defense response to injury that compartmentalizes the wood, thereby preventing the attack of fungi and insects, as well as the loss of cell moisture (Shigo 1984). The occurrence of TRD in the tree-ring records represents a valuable indicator of the existence of "hidden" scars, and can even provide information on the seasonality of events (Stoffel and Beniston 2006; Schneuwly-Bollschweiler and Stoffel 2012). In broadleaved trees, the main reaction of trees to wound damages is a significant decrease in mean vessel size within rings formed during flood conditions (Arbellay et al. 2012b; Ballesteros-Cánovas et al. 2010b).

Tilted trees are also a common feature in this region. The sudden, unidirectional pressure on the stem generated by geomorphic events (e.g., deposition of material by a debris flow) as well as the destabilization of the root-plate system by bankfull erosion cause that the stems of many trees close to the channel are rotated (Fig. 2b). Trees are responding to tilting with the formation of reaction wood (Stoffel and Bollschweiler 2008, 2009). This anatomical feature is recognized macroscopically through the occurrence of eccentric growth rings in the stem. The recognition of compression wood in the tree-ring records allows determination of the moment of tilting, and consequently dating the flood event. By using dendro-mechanical models, the magnitude of the tilting can also correlated with the flow energy and consequently provides information about the peak discharge at a given cross-section (Ballesteros-Cánovas et al. 2015c).

In the tree-ring records, growth suppression can be recognized in trees suffering from crown decapitation or stem burial (Procter et al. 2012; Kogelnig-Mayer et al. 2013). It has been reported that crown or branch losses reduce photosynthetic activity, which in turn affects the growth rate. Similarly, stem burial may prevent water supply to the roots which in turn will lead to a decrease in growth rates, although the opposite reaction has been reported as well in case when a thin layer of nutrient-rich sediments is deposited around the trunk (Kui and Stella 2016; Friedman et al. 2005).

Finally, the last botanical evidence of past floods in the Tatra Mountains is exposed roots, which are caused by bankfull failures (Osterkamp et al. 2012; Stoffel et al. 2012). Exposed roots present clear signal in the tree-ring records, reflecting sudden or continuous erosion process by noticeable changes in wood anatomy (Stoffel et al. 2013).

The large set of potential evidence coming from trees can be used in paleoflood reconstructions, but also points to differences in the intensities of different responses. Stoffel and Corona (2014) provide a detailed overview on criteria used to assign signal intensity based on the anatomical features for different species as well as on the existing indices and minimum sampling sizes. In the case of paleoflood studies, flood scars on trees are the most useful botanical indicators of paleofloods since they do not only provide information on past events with seasonal resolution,

but also represent paleostage indicators (i.e. height of the scar; Baker 2008) in flow discharge estimations (Ballesteros-Cánovas et al. 2015a).

Based on literature review (n = 52 studies performed in North America and Europe; Ballesteros-Cánovas et al. 2015b), the number of sampled trees per study was 104 ± 122 trees, of which 60 % were broadleaved trees and 40 % conifer trees.

3 Paleoflood Reconstruction in Tatra Mountain Streams Using Tree Rings

3.1 Study Site

The Tatra Mountains (Tatras) are located in the Carpathian arc (max. elevation 2655 m a.s.l.) between Poland and Slovakia. The Tatras are a crystalline and metamorphic core mountain range covered by nappes of Mesozoic sedimentary rocks. During the Pleistocene, the Tatras underwent at least three glaciations, which strongly reshaped the region, left conspicuous relief forms and moraine deposits. This mountain terrain is highly susceptible to geomorphic processes such as debris flows, snow avalanches and floods, which have caused several disasters during the last century. The study was conducted in four streams, i.e. Rybi Potok (RP), Roztoka (RS),

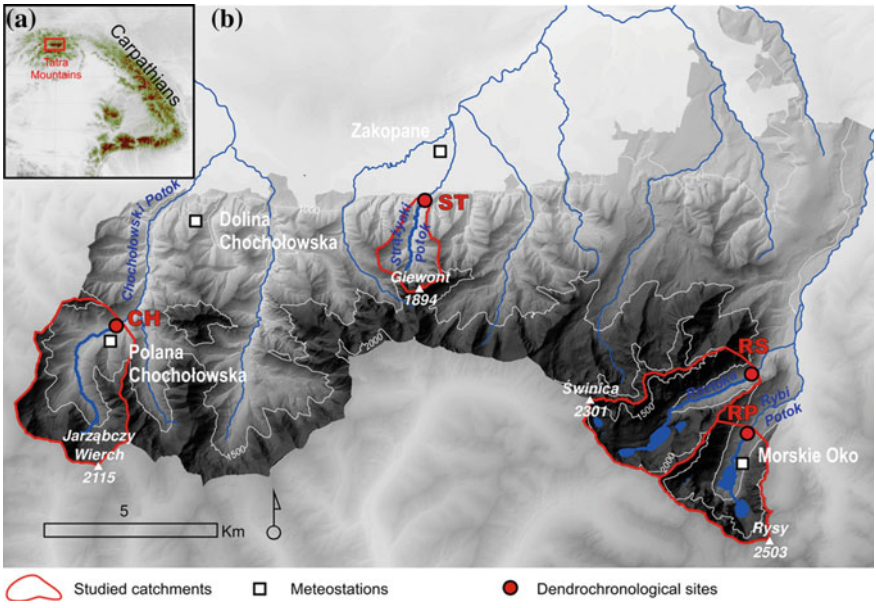

Fig. 3 **a** Location of the study site in the Carpathians. **b** Location of the investigated catchments together with meteorological stations

Strążyski (ST) and Chochołowski streams (CH), covering the western-central and eastern parts of the northern slopes of the Tatra Mountains (Fig. 3).

In this region, climate is influenced by regional air mass oscillations and local topography, with a predominance of polar marine (65 % of annual incidents) and polar continental air masses (25 %; Niedźwiedź et al. 2015). The Tatras also form a considerable barrier to air mass movements resulting in heavy rainfall events with 24-h sums of up to 300 mm (30 June 1973; Niedźwiedź 1992). Annual precipitation varies from 1100 mm at the foothills (Zakopane, 844 m a.s.l.) to 1660 mm at timberline (Hala Gąsienicowa, 1550 m a.s.l.) and 1721 mm on the summits (Lomnicky stit, 2635 m a.s.l.). The most effective precipitation events that result in flash floods are largely concentrated in the summer months as shown in Fig. 4.

Vegetation at the study sites is mostly formed by subalpine forests of Norway spruce (*Picea abies* (L.) Karst.) at higher altitudes and a mixed forest with large proportions of *P. abies*, and Silver fir (*Abies alba* Mill.) at lower altitudes. In general, stream channels are formed in gravel and loamy moraine deposits, which cover granitic and pegmatitic bedrock (Bac-Moszaszwili et al. 1979).

The land use history of the Tatras starts with Medieval ore mining, through pasturing to intense logging in the 18th and 19th centuries. The local forests have been used intensively for grazing, with peaks in grazing pressure during the 19th and mid-20th centuries, changing the characteristics of soil, vegetation, and forests, and leading to an increase in flood risk. This region has been also traditionally affected by intensive logging associated with the steel industry in the second half of the 18th century. The Tatra National Park was enacted in 1954 but pasturing locally continued until 1978 and logging remains permitted, at least in some areas of the

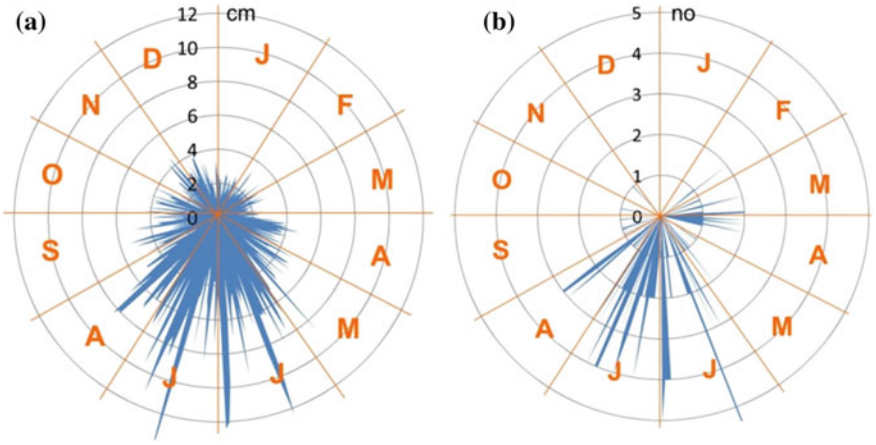

Fig. 4 Hydrometeorological situation at the northern foothills of the Tatra Mountains: **a** Average precipitation (cm) from 19 meteorological stations (28 years: 1954–1982); **b** Number of water flow larger than 1.5 times than averages as measured at Nowy Targ water gauge for the period 1898–1983 (Ballesteros-Cánovas et al. 2015a). After Ballesteros-Cánovas et al. (2015a), published by permission of Elsevier

park. The long history of timber exploitation—as fuel for the local industry and as construction material—has substantially changed the character of forests in the study region. The use of the valley floor and stream channels as transportation routes furthermore intensified this process.

3.2 Temporal Reconstruction of Floods in Tatra Mountain Streams

The reconstruction of past flood events was carried out in six representative stream sectors, previously selected due to the lack of signs of human activity or the influence by other geomorphic processes (e.g., landslides, snow avalanches). A detailed geomorphic survey and inspection of trees were performed to select trees presenting suitable past evidence of flood activity. As stated above, work focused on scars on trees due to (i) their suitability to date scars using TRDs; and (ii) the utility of scar height to estimate peak discharge. Trees growing in suitable positions (i.e. exposed to the flow) and/or with visible damage were sampled using increment borers and by following standard dendrogeomorphic sampling procedures (Stoffel and Corona 2014). Additional cores, wedges or even cross-sections were taken from dead trees. Undisturbed specimens of *P. abies* and *A. alba* were also sampled to build 5 reference chronologies. We also recorded specific information from each tree such as tree height, remarkable growth characteristics, diameter at breast height (DBH), photographs and tree location (GPS).

After field data acquisition, samples were mounted on woody supports, sanded and polished. We scanned all samples with a resolution of 3200 dpi for imagery analysis using CooRecorder and CDendro (Cybis Elektronik and Data AB; Larsson 2003a, b). The reference cores were cross-dated against site chronologies employing both visual and statistical techniques. Mistakes and growth discrepancies (i.e., missing, wedging, and false rings) were identified and corrected. Growth disturbances (GD) were analysed and dated under a stereomicroscope, with a special focus on injuries and related features such as TRDs, including their location in the tree ring, and callus tissues. Other GD such as abrupt growth suppression or release as well as the occurrence of compression wood were only used to support the interpretation of events.

The definition of flood events was based on the weighted index proposed by Kogelnig-Mayer et al. (2011), which considers the number of GD as well as their intensity for each year. The threshold used to distinguish flash flood signals from noise was set to $W_{it} \geq 0.5$ and GD ≥ 2, as suggested in previous work for hydrogeomorphic processes (e.g., Schneuwly-Bollschweiler et al. 2013).

A total of 1111 increment cores were sampled from 218 *P. abies* and *A. alba* trees affected by past flood activity. They allowed identification of 480 GD and definition of 47 flood events between A.D. 1866 and 2012 (Fig. 5). Our results reveal that the catchment presenting the largest floods activity is RP with 23

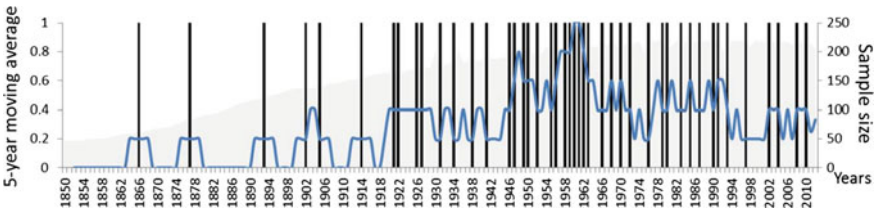

Fig. 5 Reconstructed chronology of major floods for the northern slopes of the Tatra Mountains and 5-year moving average of process activity highlighting periods of enhanced and limited flood activity. After Ballesteros-Cánovas et al. (2015a), published by permission of Elsevier

reconstructed events since A.D. 1866 (0.15 events year^{-1} with a sample size = 97), whereas the smallest activity was observed at DR with 4 reconstructed floods since A.D. 1926 (0.04 events year^{-1} with a sample size = 21). At DCH and ST, tree rings allowed the reconstruction of 19 (0.24 events year^{-1} with sample size = 73) and 9 (0.12 events year^{-1} with sample size = 22) since AD 1934 and 1938, respectively (Table 1).

Our results also suggest that a large majority of dated events (82 %) was limited to individual catchments, and no years can be found with reconstructed floods in all catchments. The flood with the largest spatial replication took place in 1970 and was documented in DCH, ST, and RP, whereas in ten other years with floods signs were found in only two catchments. The temporal occurrence of floods in the Tatras also allows distinction of at least three periods with enhanced flood activity. As shown in Fig. 5, greater activity occurred between 1946 and 1949 (5-year average: 0.8 event year^{-1}), 1955–1963 (5-year average: 0.7 event year^{-1}), and 1979–1987 (5-year average: 0.6 event year^{-1}).

3.3 Scar-Based Peak Discharge Reconstruction in Tatra Mountain Streams

After the analysis of flood occurrence in the Tatra Mountains (in terms of temporal frequency), we performed a reconstruction of flood magnitude based on a selected subset of trees presenting the most suitable evidence in the form of clear scars. The specific criteria to select the trees were (i) the presence of scars previously assigned to a specific flood event (see point 3.2); and (ii) scars facing the direction of flow and (iii) exhibiting a shape typical of flood impacts (see Ballesteros-Cánovas et al. 2010a, b for details). During fieldwork, each tree containing scars was accurately positioned with a GPS (Trimble GeoXT 6000, precision <1 m). We also measured scar height as well as the distance of trees with respect to the thalweg with a laser distance meter.

For each tree position, we computed peak discharge (q)–water stage (W) relationship W (q, i) by means of the two-dimensional hydrodynamic model

Table 1 Overview of sample size (n), growth disturbances (GD; n) and weighted index (W_{it}) for each year of the time series and for the four streams analysed

	RP			DR			DCH			ST		
Year	Sample size	N° GD	Wit	Sample size	N° GD	Wit	Sample size	N° GD	Wit	Sample size	N° GD	Wit
1866	20	2	0.66									
1877	31	4	1.39									
1893	55	2	0.94									
1903	70	3	1.21									
1905	72	2	0.52									
1914	82	3	0.68									
1921	88	4	0.66									
1922	88	6	1.00									
1926	*89*	*8*	*3.93*	*15*	*3*	*0.60*						
1927	89	7	1.96									
1931	*90*	*3*	*0.82*	*15*	*3*	*1.00*						
1934							50	2	0.54			
1938	*93*	*5*	*1.46*							*12*	*4*	*4.00*
1941							53	3	0.94			
1946							55	3	1.17			
1947										14	2	2.00
1949	94	4	0.96									
1950							58	2	0.63			
1952										15	2	1.87
1955							61	2	0.74			
1956	94	6	2.22									
1958	96	22	32.2									

(continued)

Table 1 (continued)

	RP			DR			DCH			ST		
Year	Sample size	N° GD	Wit	Sample size	N° GD	Wit	Sample size	N° GD	Wit	Sample size	N° GD	Wit
1959	*96*	*3*	*0.51*							*17*	*2*	*0.71*
1960							63	2	0.74			
1961	*96*	*5*	*0.84*				*63*	*5*	*1.19*			
1962							65	3	0.51			
1963							65	2	0.70			
1966	96	4	1.09									
1968							67	2	0.77			
1970	*96*	*4*	*0.55*				*68*	*6*	*2.86*	*19*	*2*	*1.05*
1972							70	9	8.26			
1976										21	3	2.14
1979	96	7	1.98									
1980							73	4	1.42			
1983							*73*	*3*	*0.56*	*21*	*3*	*2.43*
1985							73	3	1.19			
1987							73	4	1.36			
1990				21	3	3.00						
1991							73	2	0.93			
1993							73	2	0.56			
1997	*95*	*4*	*0.75*							*22*	*3*	*0.75*
1997												
2002	*93*	*6*	*1.43*				*73*	*6*	*1.20*			
2004				21	2	0.95						
2008	91	3	0.71									
2010										22	2	0.55

Years highlighted in italic refer to reconstructed major flood events (Ballesteros-Cánovas et al. 2015a)

IBER, which is a numerical model simulating turbulent-free, unsteady surface flows and solves depth-averaged, two-dimensional shallow water (2D Saint-Venant) equations using a finite volume method with a second-order roe scheme. In terms of digital terrain information we used LiDAR data with 1 × 1 m resolution as a basis for the mesh. Bed friction was evaluated using Manning's n roughness coefficient, which was initially assessed in the field by using homogenous roughness units (Chow 1959). In this study, we used Manning's n of 0.04 for the main channel and 0.1 for the overbank sections. To compute inlet water discharge (i.e. steady flow) into each study reach, we modelled successive inlet water discharges. At each tree, we used the best match between modelled water table and scar height to define the mean and standard deviation for the estimated average peak discharge of each flood event.

A total of 55 trees showed visible scars inflicted by sediment and/or wood transported during past flood events (namely 25 in DCH, 22 in RP, 6 in ST, and 3 in DR). Our results point out that the largest event took place in RP in 1903 with a reconstructed peak discharge of 115.9 ± 59.2 $m^3 s^{-1}$ (Table 2). By contrast, the smallest discharge of 11.1 ± 4.9 $m^3 s^{-1}$ was reconstructed for the 1934 event in catchment ST. This flood event was also dated in catchment DCH with reconstructed peak discharge of almost 39.7 ± 11.8 $m^3 s^{-1}$. On average, the range of discharges for reconstructed events was generally much higher in DCH and RP (92.8–39.7 and 115.9–28.6 $m^3 s^{-1}$, respectively) than in ST (45.8–11.1 $m^3 s^{-1}$) and DR (24.1 ± 7.6 $m^3 s^{-1}$). In terms of uncertainties related to the reconstructions, our methodology points to an average standard deviation of almost 41 %. The largest deviation (up to 80 %) was found for the 1997 event in ST, whereas the lowest deviation was observed at DCH and for an event in 1983 (∼16 %). The detailed analysis of the impact of the hydrogeomorphic position of trees used in the reconstruction suggested that the trees showing lower deviation were located: (i) in sections with straight channel configurations or on the internal side of channel bends (10–20 %), (ii) far away from neighbouring trees (23 %), or (iii) next to the boundary of bankfull channel (∼20 %). Trees showing the largest variability in scar heights were, by contrast, located on the external side of channel bends (up to 40 %), in areas with high tree density (41 %), as well as within the central channel or in overbank positions (up to 30 %).

4 Implications for Paleoflood Reconstructions in the Tatra Mountains

4.1 Climate Triggers and Flood Variability

The temporal flood reconstruction as well as the analyses of the location of TRDs within the tree rings have allowed an assessment of the seasonality of events, at least if they occurred during the growing seasons between late spring and early fall.

Table 2 Peak discharge reconstructions based on scar heights and water levels as modelled for each stream reach and each reconstructed (i.e. tree-ring data) event considered

Site	Year	Scar height (cm)	EPD (m^3/s)	RPD (m^3/s)	Site	Year	Scar height (cm)	EPD (m^3/s)	PD (m^3/s)
DCH	1934	70	48.1	39.7 ± 11.8	RP	1970	90	21.9	39.6 ± 9.5
DCH	1934	170	31.3		RP	1970	80	35.3	
DCH	1955	90	29.0	56.0 ± 23.9	RP	1903	80	74.0	115.9 ± 59.2
DCH	1955	130	45.3		RP	1903	190	157.8	
DCH	1955	90	83.7		RP	1949	140	71.8	59.4 ± 17.5
DCH	1955	90	66.1		RP	1949	40	47.0	
DCH	1963	110	69.8	92.8 ± 25.1	RP	1926	118	114.1	70.4 ± 34.6
DCH	1963	120	89.1		RP	1926	110	70.7	
DCH	1963	100	119.6		RP	1926	90	67.3	
DCH	1972	125	65.1	67.8 ± 28.9	RP	1926	50	29.7	
DCH	1972	115	83.5		RP	1958	90	52.3	86.2 ± 47.7
DCH	1972	130	58.5		RP	1958	100	47.8	
DCH	1972	50	29.2		RP	1958	90	82.1	
DCH	1972	100	39.4		RP	1958	70	162.8	
DCH	1972	155	86.1		RP	1958	120	59.5	
DCH	1972	60	113.2						
DCH	1983	120	52.3	46.7 ± 7.9	ST	1938	80	14.5	11.1 ± 4.9
DCH	1983	105	41.1		ST	1938	90	7.6	
DCH	1991	60	28	44.8 ± 23.7	ST	1947	80	14.5	20.7 ± 8.8
DCH	1991	70	61.5		ST	1947	50	53.4	
DCH	2002	30	31.2	40.4 ± 12.8	ST	1952	80	25.4	20.8 ± 6.5
DCH	2002	50	49.4		ST	1952	80	16.2	
DR	1990	85	44.8	24.1 ± 7.6					
DR	1990	40	19.1						
DR	1990	45	8.4						

EPD estimated peak discharge at each tree location; *RPD* reconstructed peak discharge for specific event (Ballesteros-Cánovas et al. 2016)

Based on a comparison with records from the closest rain gauge stations, we described the potential hydrometeorological triggers of floods by analysing the maximum 1-, 3- and 5-day April–October rainfall events. We found that for 1-day events, rainfall totals ranged from 28.8 to 168.4 mm (mean 80.2 ± 34.3 mm), whereas the 3- and 5-day precipitation sums ranged between 50.3 and 247.7 mm (mean 130.4 ± 51.3 mm) and 65.2 and 258.1 mm (mean 149.4 ± 53.5 mm), respectively (Table 2). The statistical test used (nonparametric Friedman test) confirmed the existence of non-significant differences of rainfall threshold values between the catchments. The most intense event was recorded in DCH with a daily precipitation total of 333.5 mm (24 July 1980). The most replicated event (ST, RP, DCH) occurred in 1970 and has not only been confirmed by flood records in Zakopane, but also corresponds to the second largest recorded rainfall in the Tatra Mountains on 20 July 1970, when the 1-, 3-, and 5-day accumulated rainfall totals were 150.1, 206.4, 243.2 mm, respectively (Table 3).

These results confirm the observation by Niedźwiedź et al. (2015) who suggest that rainfall above the threshold of 50 mm day^{-1} can cause floods in the Tatras (in our study we provide an average value of 80.2 mm, but with a lower minimum at 28.8 mm). The seasonality and evidence of intense daily rainfalls during May and October are in agreement with local observations and previous studies (Kotarba 2004; Niedźwiedź et al. 2015). Rain-on-snow and sudden snowmelt due to warmer springs may trigger floods as well, as stated by Zielonka et al. (2008). However, our results suggest that the main weather mechanism leading to floods is related to prolonged rainfall induced by North cyclonic circulation (Nc) (Niedźwiedź 1992; Niedźwiedź et al. 2015). This situation implies generalized and widespread occurrence of heavy rainfalls, explaining the situations with floods such as the well-replicated event of 1970, for which we observe the highest daily rainfall sums in all meteorological stations. At the same time, we also observe a large number of asynchronous flood events between catchments. While differences in catchment characteristics may play a role in flood generation, we also think that local effects, such as the presence of rainfall shadow areas (i.e. orographic effect; Borga et al. 2014) may play an important role. This hypothesis is supported by the coefficient of variation on rainfall measurement observed in rain gauge stations along the Tatra Mountains. For instance, the year 1972 was characterized by prolonged rainfall, affecting mostly the Central and Western parts of the Tatra Mountains with maximum 3-day precipitation recorded at the Hala Gąsienicowa station (218.1 mm) and reconstructed floods in catchments DCH and ST (CV:038). This rainfall shadow effect has been described for other mountain areas as well (Buytaert et al. 2006). Our results, therefore, imply that significant space-time variability exists in catchment response.

Reconstructed peak discharges confirm dissimilar catchment responses as well. The specific discharge analyses of both gauged and reconstructed flow records clearly support the observed variability of catchment responses. On the other side, we also observe that reconstructed floods from the first half of the 20th century were generally larger than those measured by the gauging stations during the second half of the century, especially in catchments ST and DCH. These observations can be explained by the evolution of land uses in the Tatra Mountains. Therefore, the strong human impact from the eighteenth to the first half of the twentieth century

Table 3 Precipitation records (1-, 3- and 5-day totals) associated with dated flash flood events

Site	Year	Likely event date	Precipitation station	1-day (mm)	3-day (mm)	5-day (mm)
DCH	1934	19.07	Historic event (no data)	N/A	N/A	N/A
DCH	1955	5.08	Dolina Chochołowska	66.4	85.2	112.2
RP	1956*	19.06	Morskie Oko	37.4	50.3	65.2
RP	1958	29.06	Morskie Oko	168.4	238.2	248.4
RP	1959	30.06	Morskie Oko	83.4	148.9	156.2
ST	1959*	1.06	Dolina Chochołowska	93.4	133.0	134.1
DCH	1960	13.07	Dolina Chochołowska	110.6	113.6	153.0
DCH	1961	30.07	Dolina Chochołowska	45.7	115.5	115.5
DCH	1962	18.07	Dolina Chochołowska	97.4	128.2	132.0
DCH	1963	5.10	Dolina Chochołowska	53.4	89.8	96.6
RP	1966	25.06	Morskie Oko	47.3	52.0	91.4
DCH	1968	18.07	Dolina Chochołowska	74.9	90.5	99.7
DCH	1970	18.07	Historic event (no data)	N/A	N/A	N/A
ST	1970	18.07	Zakopane	138.7	192.1	218.8
RP	1970	18.07	Morskie Oko	150.1	206.4	243.2
DCH	1972*	21.08	Polana Chochołowska	92.1	187.6	214.5
ST	1976	17.09	Zakopane	41.3	72.3	85.6
RP	1979*	27.06	Morskie Oko	28.8	86.3	88.5
DCH	1980	24.07	Polana Chochołowska	84.5	247.7	258.1
ST	1983	14.07	Zakopane	109.2	179.3	190.2
DCH	1983	14.07	Polana Chochołowska	84.7	118.9	134.7
DR	1990*	25.05	Morskie Oko	59.0	73.0	87.4
ST	1997	08.07	Zakopane	104.0	166.0	205.3
RP	1997	08.07	Morskie Oko	84.0	134.1	153.0

(continued)

Table 3 (continued)

Site	Year	Likely event date	Precipitation station	1-day (mm)	3-day (mm)	5-day (mm)
RP	2002	14.08	Morskie Oko	58.0	89.8	107.2
DR	2004	28.07	Morskie Oko	72.2	150.1	168.2
RP	2008	23.07	Zakopane	113.5	155.0	185.2
ST	2010	27.07	Zakopane	68.1	119.1	151.6

* represent years with a CV larger than 0.35, which indicate a larger variability in the measured precipitation over the northern slopes of the Tatra Mountains (Ballesteros-Cánovas et al. 2015a)

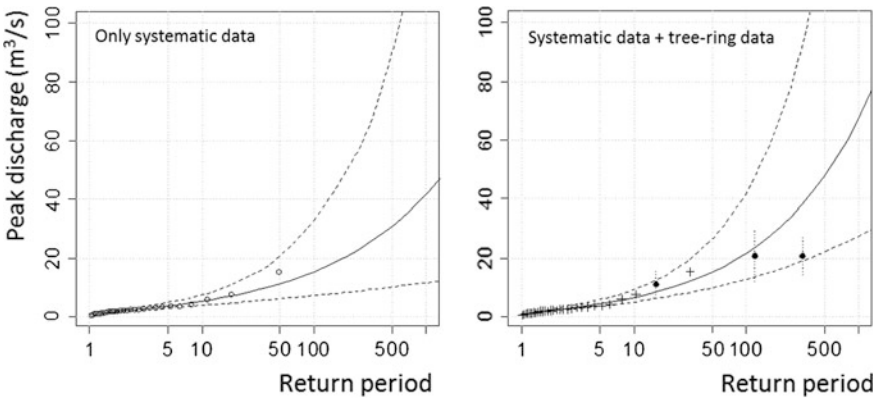

Fig. 6 Flood frequency distribution based on systematic flow gauge series (1) and the series consisting of systematic flow data and the reconstructed paleodischarges (2) After Ballesteros-Cánovas et al. (2016), published by permission of Elsevier

resulted in increased soil erosion and surface runoff, thereby favouring the formation of braided channels. Our results may also support the idea that, in general, average peak discharges could have been reduced due to the impact of intense forest recovery on runoff in the study region during the second half of the twentieth century (Wyżga et al. 2012).

4.2 Implications for Flood Hazard Assessments

The paleoflood records provided in this study have implications in terms of flood hazard definition. Despite the fact that existing historical archives describe the occurrence of intense floods triggered by summer precipitation since at least the seventeenth century (Krzemień 1991; Starkel 1996; Kotarba 2004; Gorczyca et al. 2013), the existing gauging network in the Tatra Mountains and their foreland is highly fragmented and incomplete, which therefore renders proper hazard definition and makes long-term flood studies based on systematic records very difficult. Our results provide two main outcomes which are considered very useful for an improved understanding of flood hazards in the region.

First, we provide unique and quantitative rainfall thresholds associated with long-term flood occurrences. These rainfall thresholds should be used as a baseline for the determination of probabilities of threshold exceedances under future climate conditions. By using regional climate model (RCMs) output and downscaling procedures, the expected future frequency of intense precipitation events could be compared with our data so as to provide data on changes in the duration, severity, and frequency of intense precipitation events leading to the triggering of floods in the region over the next few decades. This is specifically relevant as evidence exists

on an increase in the activity, at least in the long term, of cyclonic circulation types which are responsible for floods in the region (Niedźwiedź et al. 2015).

Secondly, the inclusion of non-systematic paleohydrological data, derived from tree-ring analysis, has an important impact on the results of the flood frequency analysis. Through the use of Bayesian Markov Monte Carlo Chain algorithms (Gaume et al. 2010; Viglione et al. 2013), we combined the reconstructed flood magnitude with the existing flow gauge series to determine changes in the flood frequency quartiles. Our results highlight that the largest changes in flood frequency (up to 25.5 % for T = 100 years) have occurred at Strążyska (ST) (Fig. 6). This implies that the flood hazard at this site would have been underestimated had the assessment of flood frequency distributions been based solely on systematic data. This finding is of high importance as the Strążyski Stream (ST) drains the catchment upslope of the main population center of the Polish Tatras, Zakopane. Consequently, our results should be taken into account for the design of hydraulic infrastructure and the definition of hazard planning. Our results also help to substantially reduce uncertainties in the estimation of the 100-year flood. Under a stochastic flood risk assessment approach, this uncertainty could be included in future risk assessments in the area, as it has been done in other regions in the past (Apel et al. 2004; Ballesteros et al. 2013).

Finally, and similarly to what is done on the southern side of the Tatra Mountains (Slovakian sector; Gáal et al. 2010), our paleoflood records could be included to deliver regional flood analysis, given that both datasets pass the homogeneity test based on the Hosking and Wallis (1997) algorithm. If so, a combined analysis on either side of the main divide could lead to a completely new setting for flood hazard assessments at the regional scale, which could then have clear and important implications for risk-based land management.

5 Conclusions

The lack of data on past floods and their impacts on the understanding of flood processes and their impacts in the Tatra Mountains and their foreland has been one of the key drivers of the FLORIST project (Kundzewicz et al. 2014b). Tree-rings studies, as the ones presented here, have been applied to Tatra Mountain streams to overcome some of the past drawbacks related with this lack of data. Despite some difficulties to deal with and to combine non-systematic (paleoflood) and systematic (gauged) records, the application of tree-ring records in Tatra Mountain streams has undoubtedly contributed to an improved understanding of past process activity, hydrometeorological triggers of floods; flood variability during the last century, and have facilitated redefinition of flood hazards in the region.

Acknowledgments This contribution has been realized in the framework of the FLORIST (Flood risk on the northern foothills of the Tatra Mountains) project, PSPB no. 153/2010, through a grant from Switzerland through the Swiss Contribution to the enlarged European Union.

References

Arbellay E, Corona C, Stoffel M, Fonti P, Decaulne A (2012a) Defining an adequate sample of earlywood vessels for retrospective injury detection in diffuse-porous species. PLoS ONE 7: e38824

Arbellay E, Fonti P, Stoffel M (2012b) Duration and extension of anatomical changes in wood structure after cambial injury. J Exp Bot 63:3271–3277

Apel H, Thieken AH, Merz B, Blöschl G (2004) Flood risk assessment and associated uncertainty. Nat Hazard Earth Syst 4(2):295–308

Bac-Moszaszwili M, Burchardt J, Głazek J, Iwanow A, Jaroszewski W, Kotański Z, Lefeld J, Mastella L, Ozimkowski W, Roniewicz P, Skupiński A, Westwalewicz-Mogilska E (1979) Mapa Geologiczna Tatr Polskich (Geological Map of the Polish Tatra), 1: 30,0000. Wydawnictwa Geologiczne, Warszawa, Poland

Baker VR (2008) Paleoflood hydrology: origin, progress, prospects. Geomorphology 101(1):1–13

Ballesteros-Canovas JA, Stoffel M, Bodoque del Pozo JM, Bollschweiler M, Hitz OM, Diez-Herrero A (2010a) Changes in wood anatomy in tree rings of Pinus pinaster Ait. following wounding by flash floods. Tree Ring Res 66:93–103

Ballesteros-Canovas JA, Stoffel M, Bollschweiler M, Bodoque del Pozo JM, Díez-Herrero A (2010b) Flash-flood impacts cause changes in wood anatomy of Alnus glutinosa, Fraxinus angustifolia and Quercus pyrenaica. Tree Physiol 30:773–781

Ballesteros-Cánovas JA, Sanchez-Silva M, Bodoque JM, Díez-Herrero A (2013) An example of integrated approach to flood risk management: the case of Navaluenga (Central Spain). Water Resour Manage 27(8):3051–3069

Ballesteros-Canovas JA, Rodriguez-Morata C, Garófano-Gómez V, Rubiales JM, Sánchez-Salguero R, Stoffel M (2014) Unravelling past flash flood activity in a forested mountain catchment of the Spanish Central System. J Hydrol. doi:10.1016/j.jhydrol.2014.11.027

Ballesteros-Cánovas JA, Czajka B, Janecka K, Lempa M, Kaczka RJ, Stoffel M (2015a) Flash floods in the Tatra Mountain streams: frequency and triggers. Sci Total Environ 511:639–648

Ballesteros-Cánovas JA, Stoffel M, St. George S, Hirschboeck K (2015b) A review of flood records from tree rings. Prog Phys Geog 1–23. doi:10.1177/0309133315608758

Ballesteros-Cánovas JA, Márquez-Peñaranda JF, Sánchez-Silva M, Díez-Herrero A, Ruiz-Villanueva V, Bodoque JM, Eguibar MA, Stoffel M (2015c) Can tree tilting be used for paleoflood discharge estimations? J Hydrol 529:480–489

Ballesteros-Cánovas JA, Stoffel M, Spyt B, Janecka K, Kaczka RJ, Lempa M (2016) Paleoflood discharge reconstruction in Tatra Mountain streams. Geomorphology 272C. doi:10.1016/j.geomorph.2015.12.004

Bollschweiler M, Stoffel M, Schneuwly DM, Bourqui K (2008) Traumatic resin ducts in Larix decidua stems impacted by debris flows. Tree Physiol 28:255–263

Borga M, Anagnostou EN, Blöschl G, Creutin JD (2011) Flash flood forecasting, warning and risk management: the HYDRATE project. Environ Sci Policy 14(7):834–844

Borga M, Stoffel M, Marchi L, Marra F, Jakob M (2014) Hydrogeomorphic response to extreme rainfall in headwater systems: flash floods and debris flows. J Hydrol 518:194–205

Brázdil R, Kundzewicz ZW, Benito G (2006) Historical hydrology for studying flood risk in Europe. Hydrol Sci J 51(5):739–764

Buytaert W, Celleri R, Willems P, Bièvre BD, Wyseure G (2006) Spatial and temporal rainfall variability in mountainous areas: a case study from the south Ecuadorian Andes. J Hydrol 329 (3):413–421

Chow V (1959) Open channel hydraulics. McGraw-Hill, New York

Friedman JM, Vincent KR, Shafroth PB (2005) Dating floodplain sediments using tree-ring response to burial. Earth Surf Proc Land 30:1077–1091

Gaál L, Szolgay J, Kohnová S, Hlavčová K, Viglione A (2010) Inclusion of historical information in flood frequency analysis using a Bayesian MCMC technique: a case study for the power dam Orlík, Czech Republic. Contrib Geophys Geodesy 40(2):121–147

Gaume E, Gaál L, Viglione A, Szolgay J, Kohnová S, Blöschl G (2010) Bayesian MCMC approach to regional flood frequency analyses involving extraordinary flood events at ungauged sites. J Hydrol 394(1):101–117

Gorczyca E, Krzemień K, Wrońska-Wałach D, Sobucki M (2013) Channel changes due to extreme rainfalls in the polish carpathians. In: Loczy D (ed) Geomorphological impacts of extreme weather. Springer, Netherlands, pp 23–35

Hosking JRM, Wallis JR (1997) Flood frequency analysis: an approach based on L-moments

Kames S, Tardif JC, Bergeron Y (2016) Continuous earlywood vessels chronologies in floodplain ring-porous species can improve dendrohydrological reconstructions of spring high flows and flood levels. J Hydrol 534:377–389

Kogelnig-Mayer B, Stoffel M, Bollschweiler M, Hübl J, Rudolf-Miklau F (2011) Possibilities and limitations of dendrogeomorphic time-series reconstructions on sites influenced by debris flows and frequent snow avalanche activity. Arctic Antarct Alp Res 43:649–658

Kogelnig B, Stoffel M, Schneuwly-Bollschweiler M (2013) Four-dimensional growth response of mature Larix decidua to stem burial under natural conditions. Trees 27:1217–1223

Kotarba A (2004) Zdarzenia geomorfologiczne w Tatrach Wysokich podczas małej epoki lodowej. (Geomorphic events in the High Tatra Mountains during the Little Ice Age) In: Kotarba A (ed) Rola małej epoki lodowej w przekształcaniu środowiska przyrodniczego Tatr (Effect of the Little Ice Age on transformation of natural environment of the Tatra Mountains). PAN IGiPZ, Kraków, pp 9–55 (in polish with english summary)

Kozlowski TT (2002) Physiological-ecological impacts of flooding on riparian forest ecosystems. Wetlands 22(3):550–561

Krzemień K (1991) Dynamika wysokogórskiego system fluwialnego na przykładzie Tatr Zachodnich. (Dynamics of the high-mountain fluvial system with the Western Tatra Mts. as example).Rozprawy Habilitacyjne (Profesure desideratum). Nr 215. Kraków. UJ. ISSN (in polish with english summary)

Kui L, Stella JC (2016) Fluvial sediment burial increases mortality of young riparian trees but induces compensatory growth response in survivors. Forest Ecol Manage 366:32–40

Kundzewicz ZW, Kanae S, Seneviratne SI, Handmer J, Nicholls N, Peduzzi P, Mechler R, Bouwe LM, Arnell N, Mach K, Muir-Wood R, Brakenridge GR, Kron W, Benito G, Honda Y, Takahashi K, Sherstyukov B (2014a) Flood risk and climate change: global and regional perspectives. Hydrol Sci J 59(1):1–28

Kundzewicz Z, Stoffel M, Kaczka R, Wyżga B, Niedźwiedź T, Pińskwar I, Ruiz-Villanueva V, Łupikasza E, Czajka B, Ballesteros-Canovas J, Małarzewski Ł, Choryński A, Janecka A, Mikuś P (2014b) Floods at the northern foothills of the Tatra Mountains—a polish-swiss research project. Acta Geophys 62(3):620–641

Larsson L-A (2003a) CooRecorder: image co-ordinate recording program. www.cybis.se

Larsson L-A (2003b) CDendro: Cybis Dendro dating program. www.cybis.se

Niedźwiedź T (1992) Climate of the Tatra Mountains. Mt Res Dev 12(2):131–146

Niedźwiedź T, Łupikasza E, Pińskwar I, Kundzewicz ZW, Stoffel M, Małarzewski Ł (2015) Variability of high rainfalls and related synoptic situations causing heavy floods at the northern foothills of the Tatra Mountains. Theor Appl Climatol 119(1–2):273–284

Osterkamp WR, Hupp CR, Stoffel M (2012) The interactions between vegetation and erosion: new directions for research at the interface of ecology and geomorphology. Earth Surf Proc Land 37:23–36

Procter E, Stoffel M, Bollschweiler M, Neumann M (2012) Exploring debris-flow history and process dynamics using an integrative approach on a dolomitic cone in western Austria. Earth Surf Proc Land 37:913–922

Schneuwly DM, Stoffel M, Dorren LKA, Berger F (2009a) Three-dimensional analysis of the anatomical growth response of European conifers to mechanical disturbance. Tree Physiol 29:1247–1257

Schneuwly DM, Stoffel M, Bollschweiler M (2009b) Formation and spread of callus tissue and tangential rows of resin ducts in Larix decidua and Picea abies following rockfall impacts. Tree Physiol 29:281–289
Schneuwly-Bollschweiler M, Corona C, Stoffel M (2013) How to improve dating quality and reduce noise in tree-ring based debris-flow reconstructions. Quat Geochronol 18:110–118
Shigo AL (1984) Compartmentalization: a conceptual framework for understanding how trees grow and defend themselves. Annu Rev Phytopathol 22(1):189–214
Shroder JF (1978) Dendrogeomorphological analysis of mass movement on Table Cliffs Plateau. Utah Quat Res 9(2):168–185
Sigafoos RS (1964) Botanical evidence of floods and flood-plain deposition. US Geol Surv Prof Pap 485A:35
Starkel L (1996) Geomorphic role of extreme rainfalls in the Polish Carpathians. Studia Geomorphologica Carpatho-Balcanica 30:21–39
Stoffel M (2008) Dating past geomorphic processes with tangential rows of traumatic resin ducts. Dendrochronologia 26(1):53–60
Stoffel M, Beniston M (2006) On the incidence of debris flows from the early Little Ice Age to a future greenhouse climate: a case study from the Swiss Alps. Geophys Res Lett 33:L16404
Stoffel M, Bollschweiler M (2008) Tree-ring analysis in natural hazards research—an overview. Nat Hazards Earth Syst Sci 8:187–202
Stoffel M, Hitz OM (2008) Snow avalanche and rockfall impacts leave different anatomical signatures in tree rings of Larix decidua. Tree Physiol 28(11):1713–1720
Stoffel M, Bollschweiler M (2009) What tree rings can tell about earth-surface processes: teaching the principles of dendrogeomorphology. Geogr Compass 3(3):1013–1037
Stoffel M, Wilford DJ (2012) Hydrogeomorphic processes and vegetation: disturbance, process histories, dependencies and interactions. Earth Surf Proc Land 37:9–22
Stoffel M, Klinkmüller M (2013) 3D analysis of anatomical reactions in conifers after mechanical wounding: first qualitative insights from X-ray computed tomography. Trees 27:1805–1811
Stoffel M, Corona C (2014) Dendroecological dating of geomorphic disturbance in trees. Tree-Ring Res 70:3–20
Stoffel M, Bollschweiler M, Butler DR, Luckman BH (eds) (2010) Tree rings and natural hazards: a state-of-art (vol 41). Springer Science & Business Media, Berlin
Stoffel M, Casteller A, Luckman BH, Villalba R (2012) Spatiotemporal analysis of channel wall erosion in ephemeral torrents using tree roots—an example from the Patagonian Andes. Geology 40(3):247–250
Stoffel M, Corona C, Ballesteros Canovas JA, Bodoque del Pozo JM (2013) Dating and quantification of erosion processes based on exposed roots. Earth Sci Rev 123:18–34
Szczepański W, Czarnecka H, Mierzwiński A (1996) Atlas posterunków wodowskazowych dla potrzeb państwowego monitoringu środowiska: posterunki wodowskazowe IMGW
Viglione A, Hosking JR, Laio F, Miller A, Gaume E, Payrastre O, Salinas JL, N'guyen CC, Halbert K (2013) Package 'nsRFA'. Non-supervised Regional Frequency Analysis. CRAN Repository. http://r.adu.org.za/web/packages/nsRFA/nsRFA.pdf
Weingartner R, Barben M, Spreafico M (2003) Floods in mountain areas—an overview based on examples from Switzerland. J Hydrol 282(1):10–24
Wohl E (2000) Mountain rivers. No. 14. Amer. Geophysical Union
Wohl E (2006) Human impacts to mountain streams. Geomorphology 79(3):217–248
Wyżga B, Zawiejska J, Radecki-Pawlik A, Hajdukiewicz H (2012) Environmental change, hydromorphological reference conditions and the restoration of Polish Carpathian rivers. Earth Surf Proc Land 37(11):1213–1226
Zielonka T, Holeksa J, Ciapała S (2008) A reconstruction of flood events using scarred trees in the Tatra Mountains, Poland. Dendrochronologia 26(3):173–183